Acta Biomaterialia 187 (2024) 98–109

Contents lists available at ScienceDirect

Acta Biomaterialia

journal homepage: www.elsevier.com/locate/actbio

Full length article

Mussel-inspired adhesive drug-loaded hydrogels for oral ulcers treatment

Zhongchao Wang[a,b,c,1], Xiao Han[d,1], Weiwei Xiao[a,b,e,1], Pin Wang[a,b,e], Jinghan Wang[a,b,e], Dan Zou[f], Xiao Luo[g], Liang Shi[a,b,e], Jiaqi Wu[a,b,e], Ling Guo[a,b,e], Yandong Mu[h,*], Bingyang Lu[d,*], Liyuan Fan[a,b,e,*]

[a] School of Stomatology, Southwest Medical University, Luzhou, Sichuan, China
[b] Oral & Maxillofacial Reconstruction and Regeneration of Luzhou Key Laboratory, School of Stomatology, Department of Prosthodontics, The Affiliated Stomatology Hospital, Southwest Medical University, Luzhou, Sichuan, China
[c] Department of Periodontics & Oral Mucosal Diseases, The Affiliated Stomatological Hospital, Southwest Medical University, Luzhou, Sichuan, China
[d] Institute of Biomaterials and Surface Engineering, Key Laboratory for Advanced Technologies of Materials, Ministry of Education, Southwest Jiaotong University, Chengdu 610031, PR China
[e] Department of Prosthodontics, The Affiliated Stomatological Hospital, Southwest Medical University, Luzhou, Sichuan, China
[f] School of Health Management, Xihua University, Chengdu, Sichuan 610039, China
[g] School of Medicine, University of Electronic Science and Technology of China, Chengdu, Sichuan, China
[h] Department of Stomatology, Sichuan Provincial People's Hospital, School of Medicine, University of Electronic Science and Technology of China, Chengdu, Sichuan, China

ARTICLE INFO

Article history:
Received 18 June 2024
Revised 6 August 2024
Accepted 22 August 2024
Available online 28 August 2024

Keywords:
Oral ulcer treatment
Adhesive hydrogel
Antibacterial and anti-inflammatory
Mussel-inspired
Drug delivery

ABSTRACT

Oral aphthous ulcers are common mucosal lesions that cause pain and discomfort. There are diverse biomaterials and drug treatments for oral ulcers used in both research and clinical settings. However, the complex oral environment often results in low adhesion and short drug retention times, which lead to poor drug availability and treatment outcomes. In this study, a mussel-inspired adhesive hydrogel was developed by grafting catechol onto hyaluronic acid (C-HA), and dopamine was added for oxidative prepolymerization to form modified hyaluronic acid (M-HA), which remarkably increased the adhesion of the hydrogels. Then, M-HA was interpenetrated into the gelatin methacryloyl (GelMA) network. Chlorhexidine gluconate (CHG) was then incorporated into the hydrogel to enhance its availability and therapeutic effect through its sustained-release capability. The GelMA/M-HA hydrogel demonstrated strong adhesion to wet tissues, antibacterial and anti-inflammatory properties, and good biocompatibility. In both rat oral ulcers and infected wounds, the adhesive hydrogel significantly accelerated the healing of the ulcers and infected wounds. These results indicated that this adhesive hydrogel offers a promising new strategy for the treatment of oral ulcers in clinical practice.

Statement of significance

Oral ulcers are a common and high-incidence mucosal condition that seriously affect people's daily lives, often making it difficult for patients to chew and speak. However, a dynamic oral environment with various types of bacteria influences drug availability and treatment effects in clinical settings. To address this challenge, an adhesive, mussel-inspired, drug-loaded hydrogel was constructed using natural macromolecules (hyaluronic acid and gelatin) with good biocompatibility. Chlorhexidine gluconate (CHG), with its broad-spectrum antibacterial activity, has been incorporated to synergistically promote oral ulcer healing. The splendid adhesion, antibacterial, and therapeutic effects of this hydrogel demonstrated a new strategy for treating oral ulcers.

* Corresponding authors.
E-mail addresses: yandongmu@126.com (Y. Mu), bingyanglu9771@gmail.com (B. Lu), fly56@swmu.edu.cn (L. Fan).
[1] These authors contributed equally to this work.

https://doi.org/10.1016/j.actbio.2024.08.038

1. Introduction

Oral aphthous ulcers are one of the most prevalent oral mucosal diseases with a high incidence (>25 % prevalence in the population) [1,2]. Uncomfortably, oral ulcers cause severe pain, which may make it difficult for patients to eat, chew, and speak, and some oral ulcers can turn into malignant diseases, such as epithelial tissue in the ulcer falling off and forming depressions [3,4]. The treatment options for oral ulcers include antibiotics and other drugs used in the whole body or parts [5]. However, the oral cavity is a complex environment that carries many functional movements, making it difficult for liquid drug preparations to remain in the affected area for a long time, resulting in low bioavailability and efficacy [6]. To address this challenge, viscous patches have been designed in recent studies [7]. Yan et al. prepared a poly(ionic liquid)-based diclofenac sodium (DS)-loaded (PIL-DS) buccal tissue adhesive patch with intrinsic antimicrobial properties that demonstrated pertinence to bacterial oral ulcers [8]. Li et al. designed a Janus patch for the accelerated treatment of oral ulcers inspired by barnacles [9]. A potentially more effective method could be drug-loaded nanoparticles, which were used to treat oral ulcer in a previous study [10]. However, these patches are capable of only a single use and it is difficult to combine this with clinical practice.

Hydrogels have a unique three-dimensional mesh structure with good biocompatibility and plasticity, which are beneficial for cell growth [11–13]. And hydrogels are versatile, providing good prospects in many fields of bioengineering, especially in controlled drug release [14–16]. Catechol is an adhesive molecule present in marine mussels, therefore, hydrogels containing catechol polymers exhibit remarkable adhesion enhancement [17,18]. Additionally, catechol has anti-inflammatory and antioxidant properties, making it suitable for use in wound healing [19–22]. Moreover, gargles of broad-spectrum antimicrobial chlorhexidine gluconate (CHG) have been proven to be useful in preventing oral mucositis caused by chemotherapy and demonstrates a healing effect on oral mucosal wounds [23,24]. On the basis of the clinical treatment means, the CHG acted in conjunction with adhesive hydrogel which can play long-term effects of the drug based on multifunctional materials and showed a better synergistic effect.

Here, we report an interpenetrating polymer network (IPN) hydrogel with the GelMA and catechol hyaluronic acid (C-HA). The GelMA was crosslinking by UV to form the backbone structure of IPN hydrogel, the dopamine (PDA) was peroxidation on the catechol of C-HA to prepare the modified hyaluronic acid (M-HA) entangle on the GelMA, the GelMA/M-HA hydrogel showed the significant adhesion property. At the same time, the CHG was loaded in the IPN hydrogel which achieved the universal antibacterial and anti-inflammatory effect. Furthermore, the effectiveness of the antibacterial and anti-inflammatory properties of the CHG/GelMA/M-HA hydrogel will also be examined in the treatment of oral ulcers. This strategy accomplishes an effective way for hydrogel dressing to treat oral ulcers in clinical.

2. Materials and methods

2.1. Materials

Hyaluronic acid (HA; 100–200 kDa), gelatin (99.0 %), methacrylic anhydride (MA, 94.0 %), and N-hydroxythiosuccinimide (NHS; 98.0 %) were purchased from Shanghai Aladdin Biochemical Technology Co. Ltd. (China). Rhodamine 123, N-(3-Dimethylaminopropyl)-N′-ethylcarbodiimide hydrochloride (EDC; ≥98 %), Dopamine hydrochloride (DA), and Phenyl (2,4,6-trimethylbenzoyl) phosphate lithium salt) (Photoinitiator LAP, >97.0 %) were purchased from Sigma-Aldrich (St Louis, MO, USA). Chlorhexidine digluconate (CHG (19–21 % water solution) and 1,1-diphenyl-2-trinitrophenylhydrazine (DPPH) were purchased from Macklin (China). *Escherichia coli* (*E. coli*; ATCC-700926) and *Staphylococcus aureus* (*S. aureus*; ATCC-6538) were provided by the Institute of Biophysics, Chinese Academy of Sciences, for bacteria-related experiments. *Porphyromonas gingivalis* (*P.gingivalis*; ATCC-33277) and *Streptococcus mutans* (*S. mutans*; ATCC-25175/35668) were provided by Southwest Medical University, China.

Trypsin (0.25 %), penicillin, streptomycin, Dulbecco's modified Eagle's medium (DMEM), high glucose DMEM, fetal bovine serum (FBS), Luria-Bertani (LB) medium, and Brain Heart Infusion (BHI) medium were purchased from Wuhan Saiweier Biotechnology Co., Ltd. (Wuhan, China). IL-1β and TNF-α Elisa kits were purchased from Jiangsu Meimian Industrial Co., Ltd. And IL-6 Elisa kits was purchased from Beijing Solarbio Science & Technology Co., Ltd.

2.2. GelMA/M-HA hydrogel preparation

The modified catechol hyaluronic acid (C-HA) has been reported in a previous study [25]. All reaction processes were maintained at a pH of approximately 4–6 through the HCl and NaOH solutions. To produce C-HA, HA (1.0 g) was dissolved in 100 mL of the MES buffer solution. To this solution, EDC (388.0 mg) and NHS (288.0 mg) were added and dissolved. The solution was allowed to rest for 30 min before 471.0 mg of dopamine was slowly added and stirred in for 4 h, this was then dialyzed for 2 d and freeze-dried. GelMA was prepared by adding MA (2.0–3.0 mL) into a gelatin water solution (10.0 g in 100 mL PBS) at 50 °C and stirred for 2 h. GelMA was then dialyzed for 7 d (50 °C) and freeze-dried until required for use. The Proton Nuclear Magnetic Resonance Spectrum (^{1}H-NMR, 400 MHz, Varianunity Inova-400 Spectrometer) was tested with D_2O dissolution and the Fourier Transform Infrared Spectrometer (FT-IR, potassium bromide pellet, Nicolet-5700 Fourier Infrared Spectrometer, Thermofisher Scientific, Waltham, MA, USA) was used to confirm the successful GelMA and C-HA synthesis.

The GelMA/M-HA combined hydrogel was prepared by combining 2 % C-HA and 4 % DA in a Tris-based buffer solution for 1 d. This allowed the polydopamine (PDA) prepolymer assemble and form M-HA, then 10 % GelMA, 1 % M-HA, and 0.2 % LAP were completely mixed and dispersed (20 % GelMA:2 % M-HA=1:1(v:v)). The mixed solution was illuminated with UV (2 mW/cm^2) for 1 min to obtain the GelMA/M-HA hydrogel. The hydrogel was freeze-dried and observed using a scanning electron microscope (SEM, Quattro S, Thermofisher Scientific).

2.3. Swelling test

The GelMA/M-HA and GelMA hydrogels (D=5 mm, H=6 mm) were immersed in PBS. The weights of the hydrogel were then measured at days 0, 1, 2, 3, 4, 5. The weight swelling rate (λ) was determined using the following equation:

$$\lambda = \frac{W_i}{W_0} \quad (1)$$

where W_i is the weight of the samples after swelling, while W_0 is the initial weight of the samples. Pictures of the hydrogel swelling before and after hydrogel swelling were recorded.

2.4. Reactive oxygen species (ROS) scavenging ability of hydrogels

The ROS-scavenging efficiency of the hydrogels was evaluated using DPPH [26]. To determine this, 200 μL of GelMA and GelMA/M-HA hydrogels were placed in a 24-well plate, then the hydrogels were immersed in DPPH (0.1 mmol/L in PBS) for 30 min. Absorbance was measured at 517 nm using a UV-vis, and the DPPH

scavenging ability was calculated using Eq. (2) as follows:

$$DPPH\ scavenging\ ability\ (\%) = \frac{A_{DPPH} - A_{Sample}}{A_{DPPH}} \times 100\% \quad (2)$$

where A_{DPPH} and A_{Sample} represent the absorbance of the DPPH solution with and without the hydrogel, respectively.

2.5. Rheological test

The rheological properties of the hydrogels were evaluated using a rheometer (Kinexus Lab +, NETZSCH, Germany). The GelMA and GelMA/M-HA hydrogels (D=25 mm, H=2 mm) were prepared to test the storage (G′) and loss modulus (G″) at 37°C. The frequency was set as 1 rad/s and the strain amplitude was set as 1 %.

2.6. Mechanical properties test

The mechanical properties of the hydrogels were tested using an electric universal testing machine (Instron 5943, Norwood, MA, USA). For the tensile properties, various hydrogels were prepared with a width of 15 mm and a thickness of 2 mm, and the testing gauge length was approximately 10 mm. To determine compression properties, various hydrogels with diameters of 12 mm and heights of 5 mm were prepared. Porcine mucous membrane and skin were chosen to analyze the availability and persistence of the hydrogels, and the adhesion strength test was based on the standard lap-shear test. Hydrogels were prepared with a diameter of 15 mm and a height of 5 mm. All the tests were performed at a constant peel speed of 10 mm/min.

2.7. Drug-loaded and releasing ability of hydrogels

Based on the method of preparation of the GelMA/M-HA hydrogel, different concentrations of CHG were mixed with M-HA, which formed total miscible liquids with GelMA and illuminated with UV for 1 min to obtain CHG/GelMA/M-HA drug-loaded hydrogels.

The CHG/GelMA/M-HA drug loaded hydrogels with 0.2 %, 0.5 %, and 1.0 % of CHG were placed into 1 mL of PBS at 37 °C. After 1, 3, 9, 12, 24, 48, 72, 96, and 144 h of soaking, 100 μL of solution was removed and its absorbance was measured at 259 nm using the microplate reader, the same volume of corresponding fresh medium was replenished.

2.8. Biocompatibility of hydrogels

Human gingival fibroblasts (hGFs) are the main cell type in the gum connective tissue, which not only has an active self-renewal ability but can also synthesize collagen fibers, elastic fibers, and mechanisms that play an important role in the protection and repair of periodontal tissues. Therefore, hGF was selected to evaluate the biocompatibility of various hydrogels. Hydrogel samples (200 μL) were inserted into 24-well plates and sterilized with a UV light. Then, 1 mL of hGFs (1×10^4 cells/mL, 10 % FBS in DMEM high-glucose medium) was added to co-culture with the hydrogel. On day 1, hGFs were evaluated for cell proliferation using CCK-8. The samples were analyzed using a microplate reader at 450 nm after the addition of CCK-8 for 3 h. Simultaneously, the samples were fixed with 2.5 % glutaraldehyde overnight, stained with rhodamine 123, and observed under a fluorescence microscope (EVOS M5000, Thermofisher).

2.9. Anti-inflammatory properties of hydrogels in vitro

Macrophages (RAW 264.7) are one of the most common inflammatory cell models widely used to evaluate the effects of inflammation and are chosen to evaluate the anti-inflammatory properties of various hydrogels. RAW 264.7 cells (2×10^5 cells/mL, 10 % FBS in DMEM high-glucose medium) were added to a 24-well plate and cultured for 24 h. Lipopolysaccharides (LPS, 50 ng/mL in DMEM cell culture medium) were added to the original culture medium and cultured for 4 h to induce inflammatory responses. The hydrogels were then immersed in DMEM for 24 h, the liquid that leached from the hydrogels were added to each well and co-cultured for 3 h. The cell culture medium was collected and analyzed using IL-1β, IL-6, and TNF-α ELISA kits, according to the manufacturer's instructions.

2.10. Antibacterial properties of hydrogels

Four types of bacteria were selected to evaluate the antibacterial properties of the hydrogels. Hydrogel samples (200 μL) were placed in 24-well plates and sterilized with UV light. The bacteria were grown in 5 mL LB (*E. coli* and *S. aureus*) and BHI (*P.gingivalis* and *S. mutans*) medium for approximately 6 h at 37 °C, respectively. The bacteria were diluted with PBS to 5×10^6 CFU/mL, and 1 mL of the solution were seeded in 24-well plates to immerse the samples. The culture was incubated at 37 °C for 24 h, the samples were taken out and washed gently by PBS. Then, 50 μL of bacterial dilution solution was coated on a plate and cultured at 37°C for 24 h. The plate was photographed to calculate the bacterial colony number using the Image J. Simultaneously, the various bacteria that adhered to the different samples were fixed with 4 % paraformaldehyde overnight and subjected to gradient dehydration by 50 %, 75 %, 90 %, and 95 % ethyl alcohol, and anhydrous ethanol for SEM observation.

For the bacteriostatic ring experiment, the four types of bacteria (50 μL, 1×10^8 CFU/mL) were coated on a plate and the hydrogel samples were place on the plates. The plate was cultured at 37 °C for 24 h. The plate was photographed, and the size of the inhibition ring was calculated using Image J.

2.11. Oral ulcer healing in vivo

All procedures were performed in accordance with the Animal Protection Agreement of the China Animal Protection Association and Southwest Medical University and all ethical guidelines for experimental animals were followed (No. 20220316-003). Sprague Dawley (SD) rats (male, 220 g) were purchased from Dossy Co., LTD (Chengdu, China). After adapting to the living environment, a filter paper (D=5 mm) soaked with acetic acid was attached to the rats' oral walls for 2 d to form the oral ulcer model. Once the ulcer was formed, the hydrogel samples were placed on the ulcer wounds. On days 1, 3, and 5 after the application of the hydrogels, photographs of the oral ulcer were recorded, and the wound area was calculated using Image J. Oral ulcer wounds and major organs (heart, liver, spleen, and kidney) were removed on day 5 and fixed with 4 % paraformaldehyde. They were embedded in paraffin and sectioned. The sections were stained with hematoxylin and eosin (H&E) and observed under a microscope.

2.12. Infected wound therapeutic efficiency in vivo

S. aureus is typically used to create an infected wound with wound seepage for bacterial inflammation. Acute skin damage was created on each of the rats back with a hole punch, to this wound, 50 μL of *S. aureus* (1×10^7 CFU/mL) was added to form an infected wound. On days 5, 10, 15, and 20, photographs of the infected wounds were recorded, and the wound area was calculated using the Image J. On day 20, the wounded tissues were removed and fixed with 4 % paraformaldehyde. Wound tissues were embedded in paraffin, sectioned, and observed under a microscope after H&E and Masson staining. Wound tissues were subjected to immunofluorescence analysis for CD68/CD206.

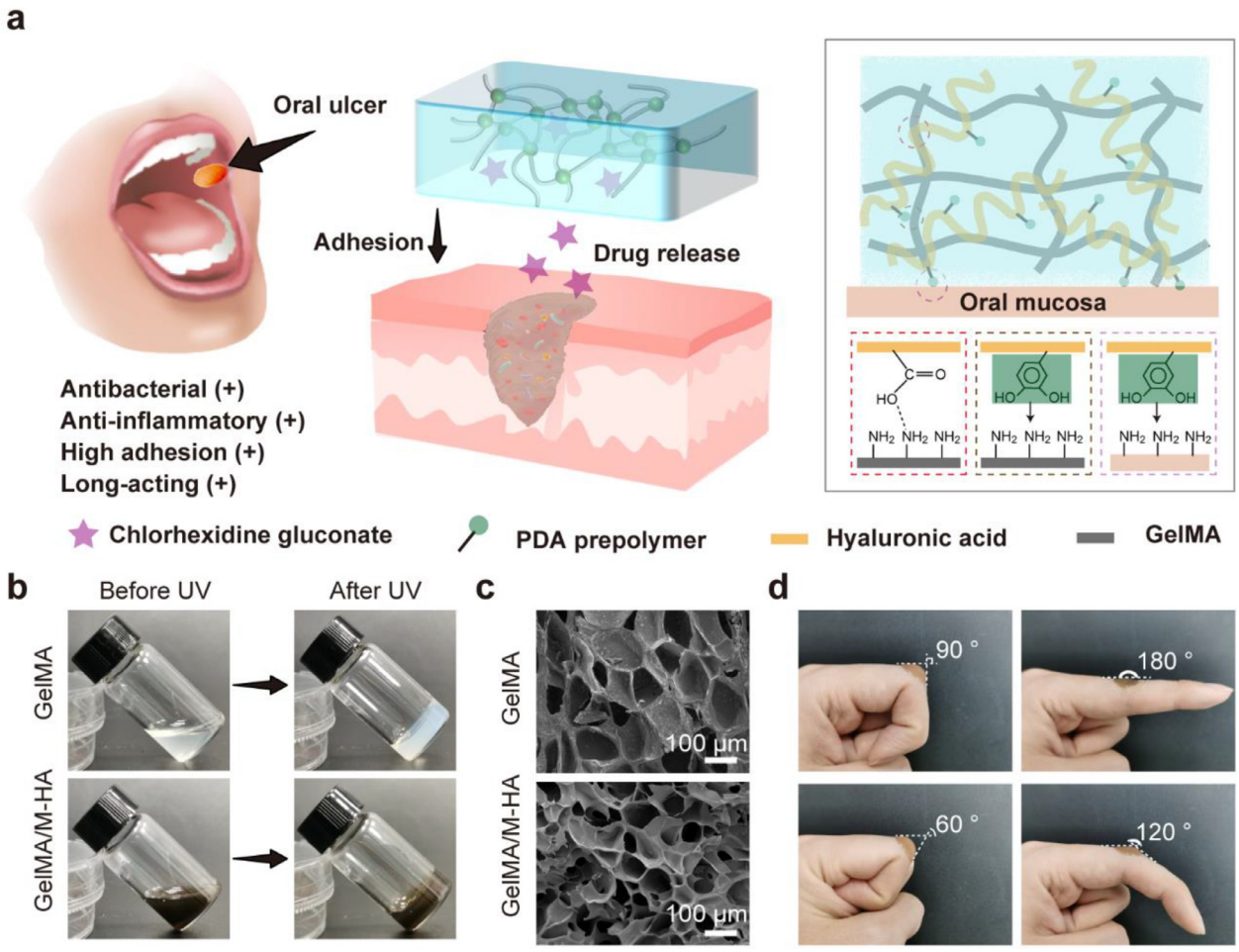

Fig. 1. Design and preparation of adhesive drug-loaded hydrogels. a Schematic of the adhesive drug-loaded hydrogels used in oral ulcers. **b** Images of GelMA and GelMA/M-HA hydrogels gelation by UV. **c** SEM images GelMA and GelMA/M-HA hydrogels. **d** Images of GelMA/M-HA hydrogels adhered on the bent finger joints under distortion stress at different angles.

2.13. Statistical analysis

All experiments were performed in triplicates, and the results are expressed as mean ± standard deviation (SD). One-way analysis of variance (ANOVA) was used to analyze the experimental results, and the statistical difference between the two groups was considered significant at $p < 0.05$.

3. Results

3.1. The characterization of the hydrogel preparation

The GelMA had mature preparation and characterization methods in recent studies [27]. The ^{1}H NMR and FT-IR spectra showed two peaks at approximately 5.5 ppm (Fig. S1a). The peak at 1725 cm^{-1} belonged to the O=C bond of Fig. S1b. The grafting rate of GelMA was approximately 50.0 %. The ^{1}H NMR and FT-IR spectra of C-HA are shown in Fig. S2, where the peak at approximately 6.75 ppm corresponds to the hydrogen proton of the benzene ring, and the peaks at 1241 cm^{-1} and 1651 cm^{-1} belong to N-C and O=C, respectively [28]. The grafting rate of C-HA is approximately 33.0 %. After 1 min UV, the GelMA and GelMA/M-HA were gelation (Fig. 1b). SEM images indicated that both the GelMA and GelMA/M-HA hydrogels had an obvious network structure, and the pore size of the GelMA/M-HA hydrogel was smaller than that of GelMA (Fig. 1c). Moreover, the GelMA/M-HA hydrogel was placed on a finger joint to observe its stability. GelMA/M-HA adhered to the finger with finger movement, whereas, GelMA was easily divorced from the finger (Fig. 1d and S3).

3.2. Physiochemical properties of the hydrogels

The anti-swelling property is critical when a hydrogel is used to treat oral ulcers. The moist environment in the oral cavity causes the hydrogel to swell easily, which influences its use. As shown in Fig. 2a, the volume of the hydrogels remained relatively constant after submergence in PBS for 5 days. The weight change of the hydrogel dipped in PBS is shown in Fig. 2b. The swelling rates of the GelMA and GelMA/M-HA hydrogels were approximately 6.0 % and 12.0 %, respectively. Based on the high GelMA hydrogel crosslinking, the anti-swelling property of the GelMA/M-HA hydrogel decreased slightly because of the hydrophilicity of HA and the UV absorption of PDA. The hydrogels reached its max swelling on day 1.

Antioxidant properties are also important for wound healing, as the inflammatory reaction is mostly accompanied by abnormal ROS [29,30]. In this study, the PDA aggregates on M-HA may have an ROS scavenging effect. DPPH was used to test the ROS-scavenging ability of the hydrogels. As shown in Fig. 2c, the GelMA/M-HA hydrogel showed a significant increase compared to that of GelMA.

Furthermore, the rheological analysis, which represented the critical state between solid and liquid, was defined as the cross

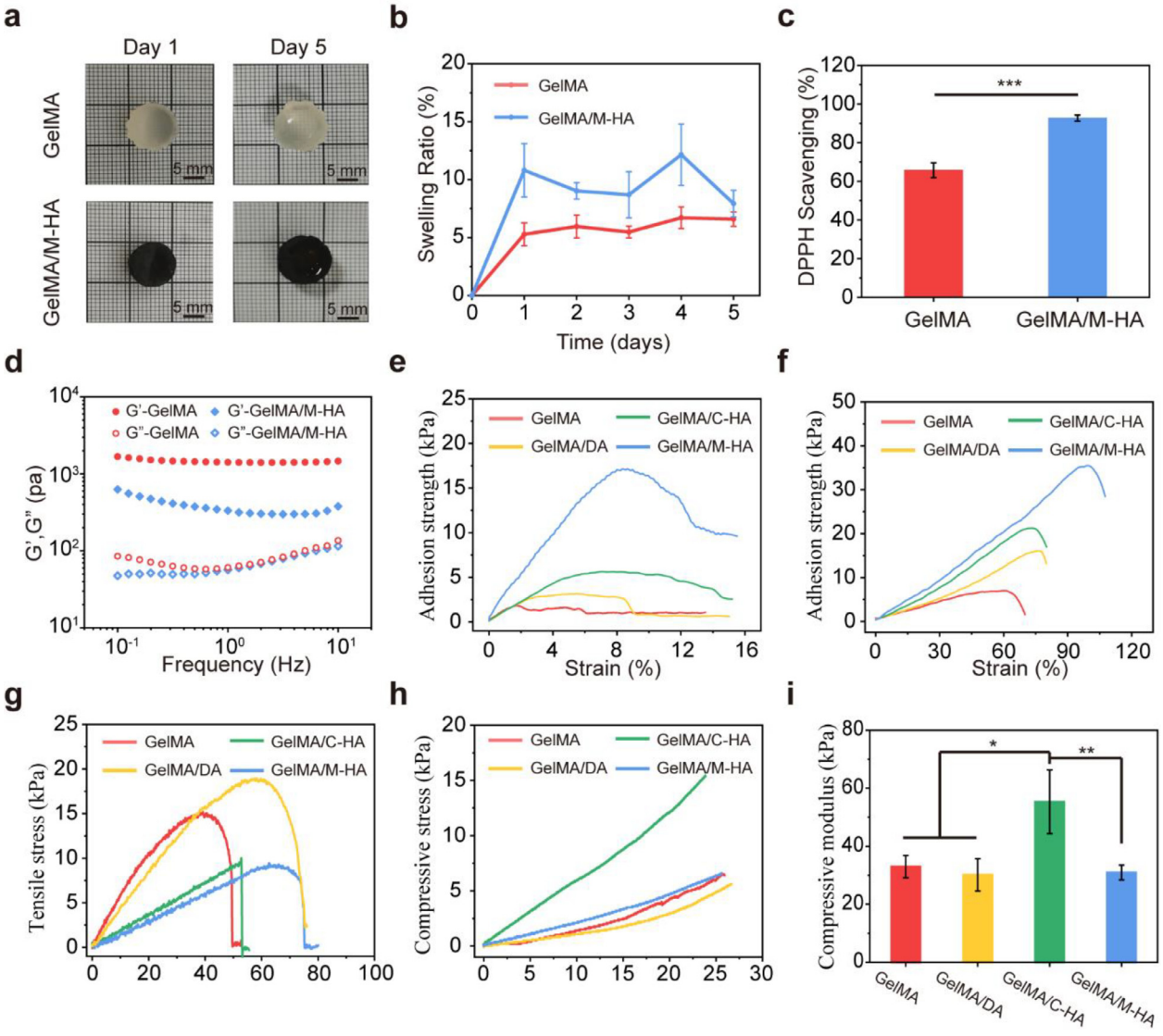

Fig. 2. Physiochemical properties of adhesive hydrogels. a Images of GelMA and GelMA/M-HA hydrogels swelling at day 1 and 5. **b** Swelling ratio curve of GelMA and GelMA/M-HA hydrogels. **c** ROS inhibiting of GelMA/M-HA hydrogels for DPPH free radical. **d** Storage and loss moduli (G' and G") of GelMA and GelMA/M-HA hydrogels. **e** Shear adhesion strength curve of various hydrogels on porcine skin. **f** Shear adhesion strength curve of various hydrogels on porcine mucosa. **h** Tensile stress curve of different hydrogels. **g** Compressive stress curve of different hydrogels. **i** Compressive modulus of different hydrogels. (n=5, $^{*}p < 0.05$, $^{**}p < 0.01$, $^{***}p < 0.001$).

point of G′ and G″. As shown in Fig. 2d, the G′ of GelMA/M-HA hydrogel was lower than GelMA, however, both hydrogels had a similar G″ at a high vibration frequency. This result indicated that the GelMA/M-HA hydrogel was more suitable for oral adhesion than GelMA.

Considering the complex and variable oral environment, the adhesive and mechanical properties of the hydrogels were systematically determined to maintain a stable state of adherence to the oral mucosa [7]. In this study, DA was mixed into the solution before GelMA hydrogel gelation (GelMA/DA), and C-HA and GelMA were mixed to form GelMA/C-HA. Conversely, the hydrogel adhesion was evaluated with porcine skin. The adhesive strength between GelMA/M-HA hydrogel and porcine skin was significantly increased for the M-HA incorporation, with an adhesive strength of 16.52 kPa, which was approximately 7.90 times greater than that of the GelMA hydrogel, as this only had an adhesive strength of 2.09 kPa (Fig. 2e and S4a). In contrast, the porcine buccal mucosa was adhered to various hydrogels, and the shear adhesive strength was tested using a universal mechanical test machine, as shown in (Fig. 2f and S4b). The adhesive strength between the GelMA/M-HA hydrogel and the mucosa was approximately 28.52 kPa, whereas that of GelMA was 7.42 kPa. Although the adhesive abilities of GelMA/DA and GelMA/C-HA were higher than that of GelMA, they were remarkably lower than that of the GelMA/M-HA hydrogel. This result indicates that PDA pre-polymerization in the hydrogel resulted in stronger adhesion than compared to the others.

Tension and compression properties were measured to assess the mechanical properties of the hydrogels. The tensile curves are shown in Fig. 2g and S4c, it indicates that the HA incorporated in the hydrogel improved the ductility of the hydrogel, which verified that HA was entangled in the network of hydrogels to form an interpenetrating polymer network. The addition of DA decreased the tensile strength, which might be caused by the DA absorption of UV or its black influence on UV-stimulated gelation. Simultaneously, the compression properties of GelMA/C-HA were better than those of the others, and its compression modulus was the highest, as shown in Fig. 2h and i. The mechanical properties of the

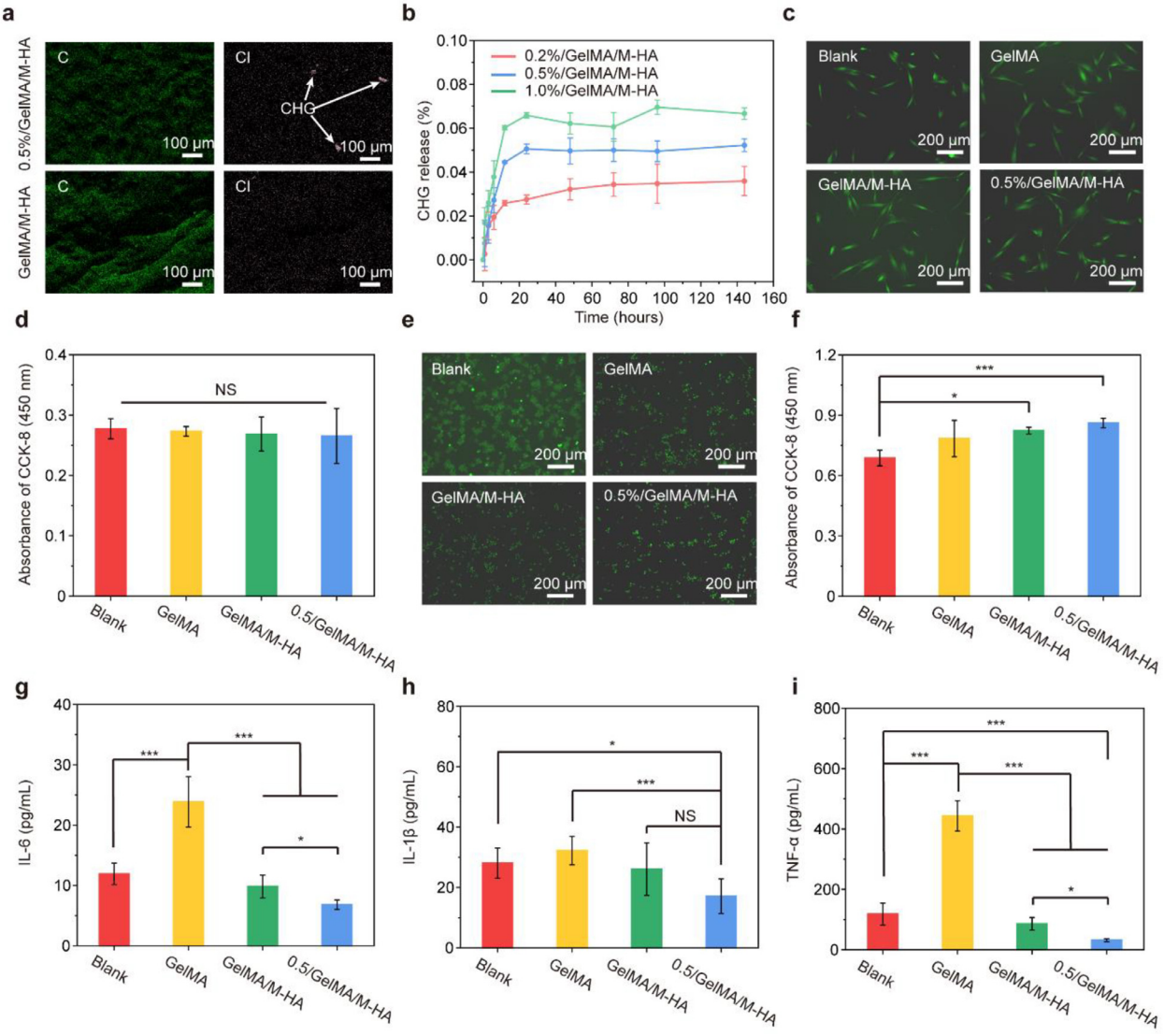

Fig. 3. Drug release of hydrogels and biological properties. a SEM-EDS images of drug-loaded GelMA/M-HA hydrogels. **b** CHG release curve of GelMA/M-HA hydrogels with different concentrations. **c** Fluorescence images of rhodamine 123 stained hGFs co-cultured with different hydrogels at day 1. **d** CCK-8 of the viability of hGFs co-cultured with different hydrogels at day 1. **e** Images of rhodamine 123 stained macrophages induced by LPS and regulated by different hydrogels. **f** CCK-8 of the viability of macrophages induced by LPS and regulated by different hydrogels. **g** IL-6 release from macrophages regulated by different hydrogels. **h** IL-1β release from macrophages regulated by different hydrogels. **i** TNF-α release from macrophages regulated by different hydrogels. (n=3, $^{*}p < 0.05$, $^{**}p < 0.01$, $^{***}p < 0.001$).

GelMA/M-HA hydrogel were soft and malleable, in accordance with the rheological results.

3.3. Drug-releasing ability of the hydrogels

The vital significance of hydrogels as wound dressings is their sustained drug release and improved drug availability. CHG was loaded onto the GelMA/M-HA hydrogel at different concentrations (0.2 %, 0.5 %, and 1.0 %). SEM and energy dispersive X-ray spectroscopy (EDS) showed that the Cl of the CHG condensate appeared in 0.2 %/GelMA/M-HA, which indicated that CHG was successfully loaded into the hydrogel (Fig. 3a). Elemental analysis showed that Cl increased from 0.3 % to 1.4 % when CHG was loaded (Fig. S5). The drug-release curve for the drug-loaded GelMA/M-HA hydrogel is shown in Fig. 3b (the standard curve is shown in Fig. S6). Within 12 h, the drug release concentration increased rapidly. The drug concentrations remained stable for 144 h. However, a medium CHG concentration can achieve the same or higher drug release, which affects drug bioavailability. The electrically charged group of CHG was ionized in the solvent, which combined with the group of hydrogels to aggregate the floccules, resulting in incomplete gelation of the hydrogel. Therefore, 0.5 %/GelMA/M-HA was selected to conduct follow-up experimentation to ensure the effectiveness of the drug.

3.4. The compatibility and anti-inflammatory properties of the hydrogels

HGFs are representative oral mucosal cells involved in wound healing [11]. In the fluorescence microscopy images, the hGFs stained with rhodamine 123 showed that all groups had a similar number of hGFs and the hGFs on the hydrogels had a better spread (Fig. 3c). CCK-8 analysis showed that the hydrogel samples had no impact on hGFs proliferation (Fig. 3d).

Subsequently, macrophages (RAW 264.7) were used to invoke an inflammatory response [31]. Various hydrogels have been pre-

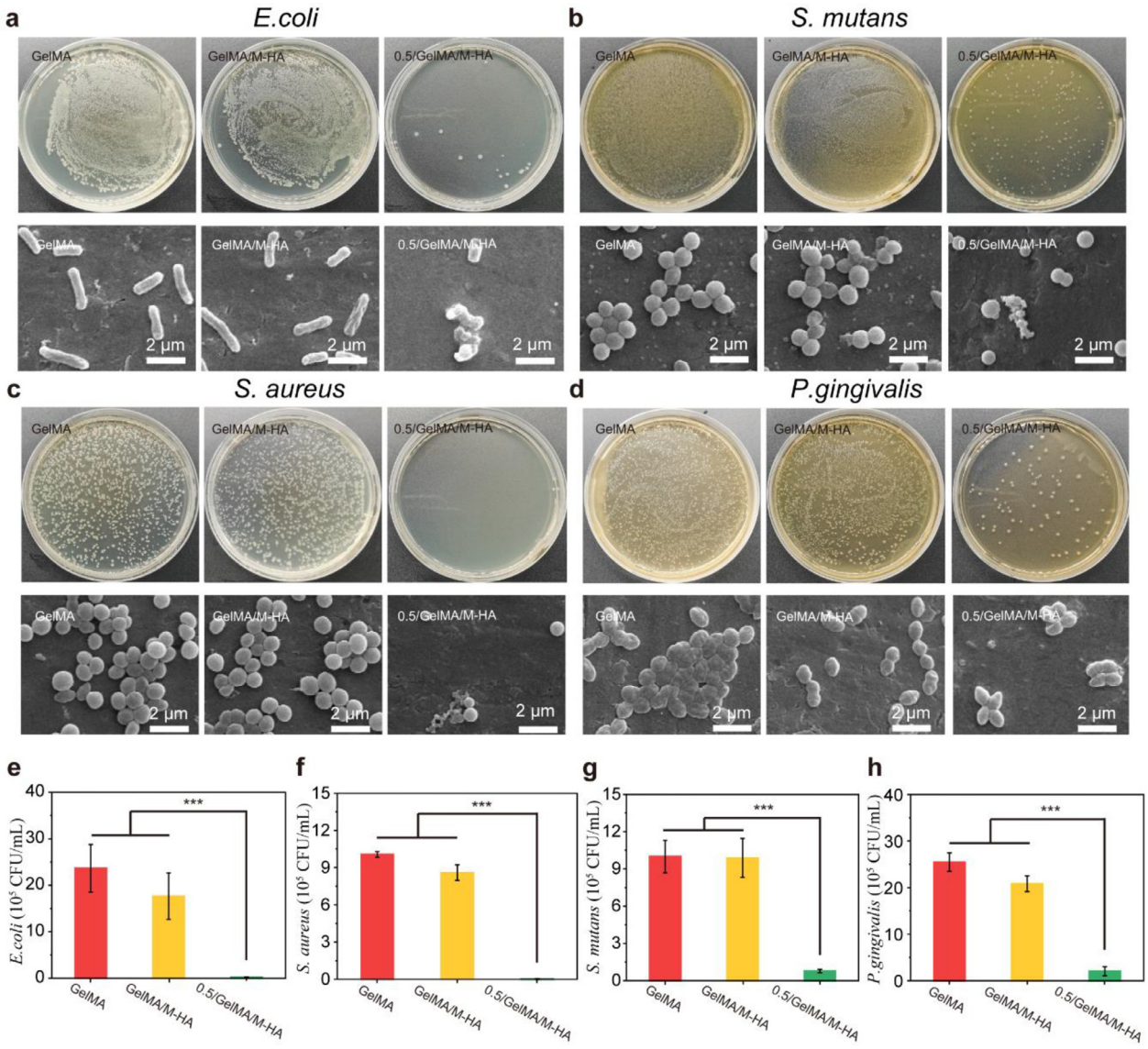

Fig. 4. Anti-bacterial properties of hydrogels. a Images of *E.coli* colonies and SEM of *E.coli* co-cultured with hydrogels. **b** Images of *S.mutans* colonies and SEM of *S.mutans* co-cultured with hydrogels. **c** Images of *S.aureus* colonies and SEM of *S.aureus* co-cultured with hydrogels. **d** Images of *P.gingivalis* colonies and SEM of *P.gingivalis* co-cultured with hydrogels. **e** Number of the *E.coli* co-cultured with hydrogels. **f** Number of the *S.aureus* co-cultured with hydrogels. **g** Number of the *S.mutans* co-cultured with hydrogels. **h** Number of the *P.gingivalis* co-cultured with hydrogels. (n=3, $^{*}p < 0.05$, $^{**}p < 0.01$, $^{***}p < 0.001$).

pared with their extract liquids in the culture medium, and the extract liquids have been used to regulate macrophages with an inflammatory response. Macrophages were stained with rhodamine 123 (Fig. 3e). Macrophages induced by LPS were round and pancake-like (blank group), which proved that the macrophages differentiated into M1 phenotypes [32]. However, the macrophages co-cultured with the hydrogel were regulated, and their phenotype was not obvious in M1. CCK-8 analysis showed that the hydrogel extract liquids co-cultured with macrophages exhibited higher proliferative activity than that of the blank group (Fig. 3f). Furthermore, inflammatory factors IL-1β, IL-6, and TNF-α were tested to analyze the inflammatory response [33–35]. As shown in Fig. 3e–i, the secretion of the inflammatory factor GelMA was higher than that of the blank because of the low cell activity of the blank group. The 0.5 %/GelMA/M-HA had the lowest inflammatory factor release than others, while it had the highest cell activity. All three inflammatory factors are pro-inflammatory factors that are secreted by M1. The significant reduction in their levels in the 0.5 %/GelMA/M-HA group supports the results of its anti-inflammatory properties. In addition, the levels of proinflammatory factors released by GelMA/M-HA decreased with the addition of PDA.

3.5. Antibacterial properties of the hydrogels

CHG is widely used for its broad-spectrum antibacterial properties in clinical. Therefore, typical gram-negative bacteria (*E.coli*), gram-positive bacteria (*S. aureus*), *P.gingivalis,* and *S. mutans* were used to test the antibacterial properties of the hydrogels. After being co-cultured with the various hydrogels, the four types of bacteria adhered to and proliferated in the hydrogel and bacterial culture medium; only in the 0.5 % CHG loaded GelMA/M-HA group did the bacterial activity decrease until death occurred (Fig. 4a–d). The 0.5 %/GelMA/M-HA hydrogel exhibited outstanding antibacterial properties against *E.coli, S. aureus, P.gingivalis,* and *S. mutans*. Thus, it is possible that the 0.5 %/GelMA/M-HA drug-loaded hydrogel has a universal antibacterial effect. SEM analysis of the morphology of the bacteria adhered to the hydrogels, as shown in

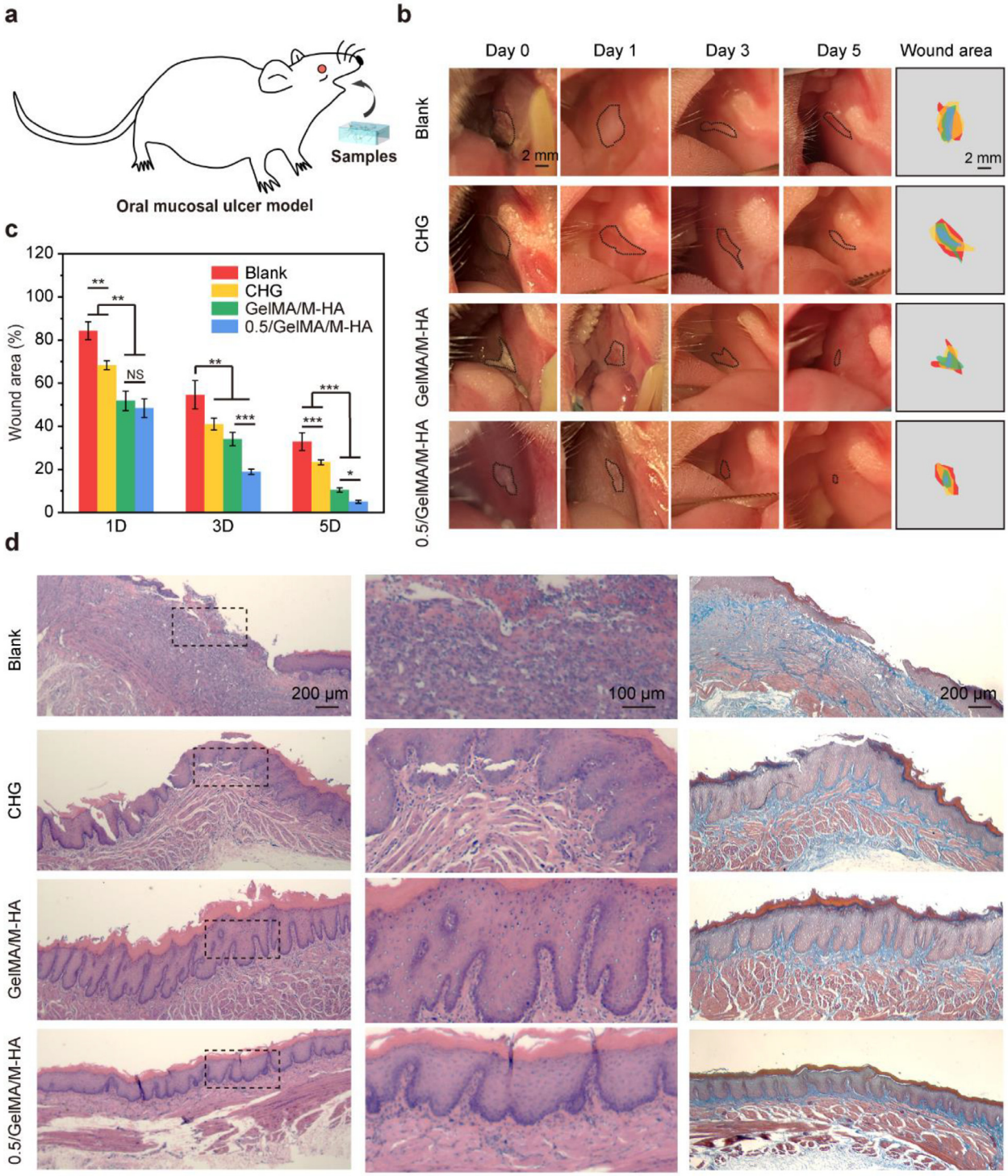

Fig. 5. Adhesive drug-loaded hydrogels for oral ulcer treatment. a Schematic of hydrogels used in oral ulcer treatment. **b** Images of oral ulcer treatment in different ways at day 0, 1, 3, and 5. **c** Wound area of the oral ulcer at day 1, 3 and 5. **d** HE and Masson staining of oral ulcer treated by different ways at day 5. (n=5, $^{*}p < 0.05$, $^{**}p < 0.01$, $^{***}p < 0.001$).

Fig. 4a–d, it showed that the bacteria had a full and smooth appearance in the GelMA and GelMA/M-HA hydrogels. However, in the 0.5 %/GelMA/M-HA hydrogel, the bacteria were depressed or crumpled, and some types of bacteria could not maintain their original form for granulation. The bacterial concentration calculated by bacterial coating (Fig. 4e–h), showed that bacterial growth in GelMA and GelMA/M-HA was unaffected. However, the bacterial growth in the 0.5 %/GelMA/M-HA hydrogel was decreased, approximately 67.8, 661.3, 10.3, and 12.6 times for *E.coli, S. aureus, P.gingivalis*, and *S. mutans,* respectively. In addition, except *S. mutans*, the GelMA/M-HA hydrogel exhibited slight antibacterial activity. This might be because the concentration of the bacterial culture solution was higher; therefore, the antibacterial ability of the catechol group was insufficient, and some of the CHG was significant.

A bacteriostatic ring experiment was performed to analyze the antibacterial activity of the hydrogels. As shown in Fig. S7, all four bacteria were restrained by CHG, and the diameters of the bac-

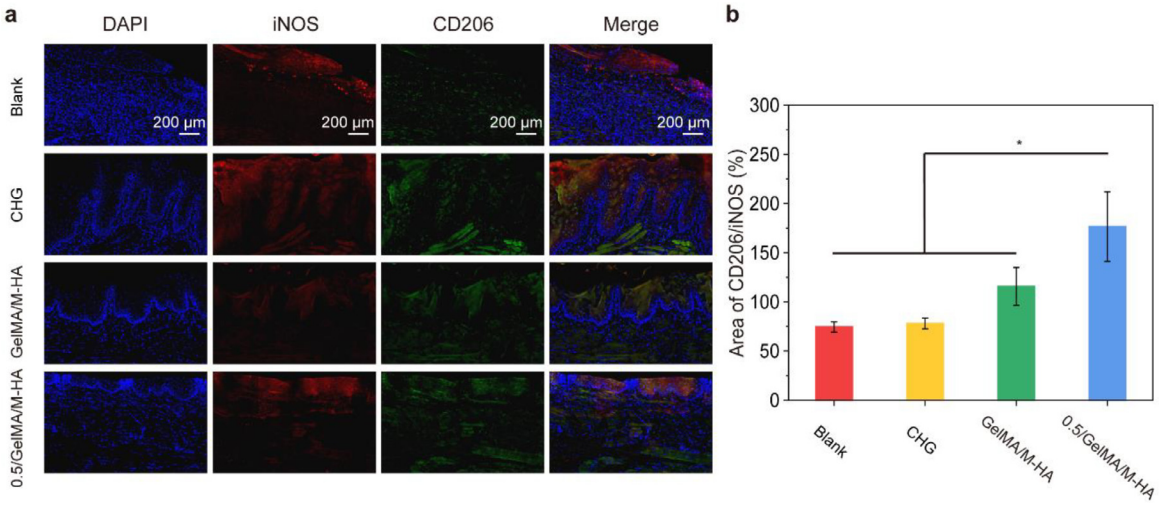

Fig. 6. Immunofluorescence staining for oral ulcer treatment. a Immunofluorescence staining images of oral ulcers treatment in different ways at day 5. **b** The fluorescence area of CD206/iNOS at day 5. (n=3, $^{*}p < 0.05$, $^{**}p < 0.01$, $^{***}p < 0.001$).

teriostatic circles were noticeably increased by approximately 4.4, 5.9, 3.0, and 9.6 times for *E.coli, S. aureus, P.gingivalis*, and *S. mutans,* respectively. When the concentration of CHG increased to 1.0 %, the bacteriostatic cycle expanded.

3.6. *Oral ulcers healing* in vivo

To further investigate oral ulcer healing *in vivo*, an oral ulcer model was constructed in rats to evaluate the process and speed of healing with different hydrogel treatments (Fig. 5a). The healing process was recorded with a picture, as shown in Fig. 5b, and images of the oral ulcers were used to analyze the size using Image J. On day 1, the hydrogel dressing promoted oral ulcer healing compared to the blank and CHG mist spray groups, although the CHG mist spray group also received oral ulcer therapy. On days 3 and 5, the 0.5 %/GelMA/M-HA hydrogel exhibited the best treatment effect, and the wound area was significantly reduced (Fig. 5c). The wound area analysis showed that the adhesive GelMA/M-HA hydrogel promoted the healing of oral ulcers because of its long-term retention and sustained drug release. Thus, CHG plays a vital role in the GelMA/M-HA hydrogel drug delivery system. On day 5, H&E staining of the oral ulcer wound was conducted (Fig. 5d). It was observed that only the 0.5 %/GelMA/M-HA hydrogel-treated group had an intact and thin epidermis. Moreover, the number of inflammatory cells on the oral ulcer was minimal in oral ulcer treated with 0.5 %/GelMA/M-HA hydrogel. Masson's staining showed that the 0.5 %/GelMA/M-HA hydrogel group exhibited the best treatment results. The oral ulcers were also stained by immunofluorescence with iNOS (red) and CD206 (green) (Fig. 6a and S8) and immunohistochemistry with IL-6/TNF-α (Fig. S9), illustrating that the 0.5 %/GelMA/M-HA hydrogel treatment group had significant inflammatory regulation (Fig. 6b).

Regarding oral use, it is inevitable that the hydrogel has a risk of being swallowed by a living body. The viscera (heart, liver, spleen, lung, and kidney) of rats treated with the hydrogel were observed after H&E staining for histological assessment. As shown in Fig. S10, the hydrogel dressings caused no damage to these organs, indicating that the hydrogel has good biosafety and biocompatibility.

3.7. *Infected wound healing* in vivo

To further explore the universality of wound healing with hydrogels, an infected wound model was constructed on the backs of rats. The hydrogels were attached to the infected wounds. As shown in Fig. 7a, the images of the infected wound healing process show that the 0.5 %/GelMA/M-HA hydrogel had the best wound healing. The wound area statistics using Image J showed that the CHG spray group promoted healing in the early stage, and the 0.5 %/GelMA/M-HA hydrogel showed conspicuous treatment (Fig. 7b). Moreover, the GelMA/M-HA hydrogel indicated that the hydrogel without CHG also promoted infected wound healing compared to that of the other groups.

On day 20, H&E staining of the healing-infected wound was intuitively displayed on the wound edge (Fig. 7c and f). The results demonstrated that the 0.5 %/GelMA/M-HA hydrogel decreased the wound to approximately 3700 μm from 6900 μm. The number of angiogenesis treated with 0.5 %/GelMA/M-HA was approximately 1.8 times than that in the other groups (Fig. 7d and g). Through Masson staining, the collagen volume fraction (CVF) was used to assess infected wound healing, as shown in Fig. 7e and h. Wounds treated with the 0.5 %/GelMA/M-HA hydrogel were approximately 86.7 % healed, which was higher than that of the other groups. On day 5, the unhealed wounds were stained with CD68/CD206 to analyze the MA phenotype (Fig. S11). The results showed that the M2 phenotype was the main component of MA in the 0.5 %/GelMA/M-HA treated group, which indicated that inflammation in chronic wounds was regulated by 0.5 %/GelMA/M-HA. All the results showed that the infected wound promoted healing using the 0.5 %/GelMA/M-HA hydrogel.

4. Discussion

The oral ulcer is an obnoxious oral wound disease, the vital clinical need is rapid healing when the clinical treatment is insufficient to meet demand such as some sprays and regular patches [36], therefore, there is a need for more effective strategies for the treatment of oral ulcers. To address the treatment challenges and clinical needs of oral ulcers, hydrogels are a very promising treatment with wet tissue adhesion and improved drug delivery [37–39]. The two irreplaceable advantages of adhesive hydrogels are the sustained-release ability of therapeutic drugs and long-term local action ability, as well as the biocompatibility and biofunctionality of the hydrogel materials [40,41]. To achieve these required characteristics, inspiration has been taken from the marine mussel, as mussel-inspired catechol hydrogels present outstanding adhesive capacity and antioxidant and anti-inflammatory effects [19]. However, the capabilities of these hydrogels can be improved. To

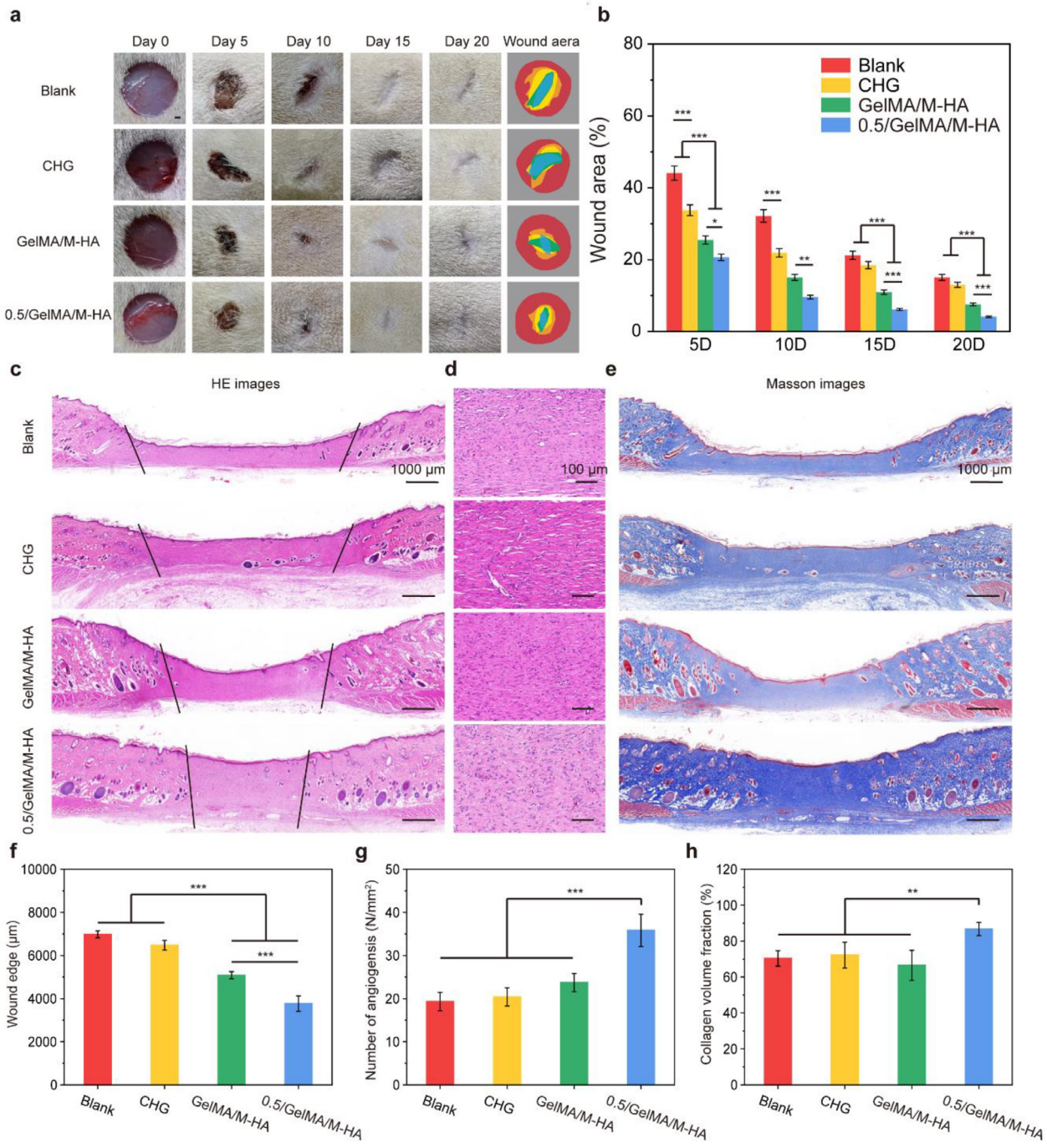

Fig. 7. Adhesive drug-loaded hydrogels for infected wound treatment. a Images of infected wound treatment in different ways at day 0, 5, 10, 15, and 20 (Scale bar=1 mm). **b** Wound area of the infected wound at day 5, 10, 15, and 20. **c** HE staining of an infected wound treated in different ways at day 20. **d** HE staining of angiogenesis in different ways at day 20. **e** Masson staining of an infected wound treated in different ways at day 20. **f** Statistical graph of wound edge at day 20. **g** Statistical graph of angiogenesis at day 20. **h** Statistical graph of CVF at day 20. (n=3, $^{*}p < 0.05$, $^{**}p < 0.01$, $^{***}p < 0.001$).

further improve adhesion, DA was added and pre-polymerized in the hydrogel, which increased the degree of substitution of catechol groups and loaded into the hydrogels [42–44]. The adhesion ability of GelMA/M-HA was higher than those of GelMA/C-HA and GelMA/DA. By adjusting the pre-polymerization time, the adhesive ability increased (Fig. S12). This illustrates that oxidation or formation of polydopamine can increase the adhesion of the hydrogel. However, cohesion and interpenetration of the hydrogel supported its increased adhesion ability. To analyze the mechanical properties of the hydrogel, it was acknowledged that the addition of HA and the color change for DA polymerization softened the GelMA/M-HA hydrogels [19,45]. However, the intermolecular interactions between HA, catechol, and GelMA improve physical crosslinking [46,47]. Interestingly, the soft GelMA/M-HA hydrogel showed better suitability and higher adhesive ability in the oral mucosa.

Although the catechol group showed a tendency to promote healing, antibacterial and anti-inflammatory effects, it was not sufficient or remarkable when used in severe wounds or excess bacteria. Individual drugs have low bioavailability, making long-term retention in the wound area difficult. This reflects the need to design a combined system with a drug and bioactive materials to achieve

better treatment. Therefore, CHG was loaded into the hydrogel to demonstrate a significant advantage over the clinical CHG mist spray. Both drug availability and therapeutic effects were improved when CHG was loaded into the hydrogel. It promoted wound healing, antibacterial, and anti-inflammatory effects [48]. Thus, in this study, the CHG load and catechol functionalization of the hydrogel had an obvious synergistic effect in promoting wound healing. Furthermore, this adhesive hydrogel was used to load other drugs into various microenvironments and wounds.

5. Conclusion

In this study, a CHG-loaded hydrogel was designed with improved wet-tissue adhesion and sustained-release drug capabilities. Natural macromolecular GelMA was chosen for the hydrogel skeleton, and HA was chosen to form an interpenetrating network in which the two macromolecules had good biocompatibility. The catechol groups grafted on HA supported the wet tissue adhesion ability, and CHG promoted healing and antibacterial and anti-inflammatory effects. Thus, CHG/GelMA/M-HA is a better treatment for oral ulcers and infected wounds *in vivo*. It is anticipated that this hydrogel design will contribute to alleviating oral ulcers.

Declaration of competing interest

The authors declare that they have no known competing financial interests or personal relationships that could have appeared to influence the work reported in this paper.

CRediT authorship contribution statement

Zhongchao Wang: Writing – original draft, Visualization, Validation, Project administration, Methodology, Formal analysis, Conceptualization. **Xiao Han:** Writing – original draft, Methodology, Formal analysis, Data curation. **Weiwei Xiao:** Methodology, Formal analysis, Data curation. **Pin Wang:** Methodology, Formal analysis. **Jinghan Wang:** Formal analysis. **Dan Zou:** Writing – review & editing. **Xiao Luo:** Visualization. **Liang Shi:** Methodology. **Jiaqi Wu:** Validation. **Ling Guo:** Methodology. **Yandong Mu:** Validation, Supervision, Resources. **Bingyang Lu:** Writing – review & editing, Visualization, Supervision, Conceptualization. **Liyuan Fan:** Writing – review & editing, Visualization, Validation, Resources, Funding acquisition, Conceptualization.

Acknowledgments

This work was supported by the Sichuan Animation Research Center (grant No. DM202118), Affiliated Stomatological Hospital, Southwest Medical University (grant No. 2023DS08), Opening Fund of Harmful Components and Tar Reduction in Cigarette Key Laboratory of Sichuan Province (grant No. jykf202205) and Chengdu Science and Technology Project (grant No. 2024-YF09-00026-SN).

Supplementary materials

Supplementary material associated with this article can be found, in the online version, at doi:10.1016/j.actbio.2024.08.038.

References

[1] Z. Slebioda, E. Szponar, A. Kowalska, Etiopathogenesis of recurrent aphthous stomatitis and the role of immunologic aspects: literature review, Arch. Immunol. Ther. Exp. 62 (3) (2014) 205–215.
[2] T. Dudding, S. Haworth, P.A. Lind, et al., Genome wide analysis for mouth ulcers identifies associations at immune regulatory loci, Nat. Commun. 10 (2019) 1052.
[3] C. Scully, S. Porter, Oral mucosal disease: recurrent aphthous stomatitis, Br. J. Oral Maxillofac. Surg. 46 (3) (2008) 198–206.
[4] X. Zeng, X. Jin, L. Zhong, G. Zhou, M. Zhong, W.M. Wang, Y. Fan, Q. Liu, X.M. Qi, X.B. Guan, Z.M. Yan, X.M. Shen, Y.F. Wu, L.J. Fan, Z. Wang, Y. He, H.X. Dan, J.T. Yang, H. Wang, D.J. Liu, H. Feng, K. Jiao, Q.M. Chen, Difficult and complicated oral ulceration: an expert consensus guideline for diagnosis, Int. J. Oral Sci. 14 (1) (2022) 28.
[5] M. Schemel-Suárez, J. López-López, E. Chimenos-Küstner, Oral ulcers: differential diagnosis and treatment, Med. Clin. 145 (11) (2015) 499–503.
[6] M. Avila, D.M. Ojcius, Ö. Yilmaz, The oral microbiota: living with a permanent guest, DNA Cell Biol. 28 (8) (2009) 405–411.
[7] C.Y. Cui, L. Mei, D.Y. Wang, P.F. Jia, Q.H. Zhou, W.G. Liu, A self-stabilized and water-responsive deliverable coenzyme-based polymer binary elastomer adhesive patch for treating oral ulcer, Nat. Commun. 14 (1) (2023) 7077.
[8] Z.J. Zhang, Q.Y. Zhang, S.A. Gao, H. Xu, J.N. Guo, F. Yan, Antibacterial, anti-inflammatory and wet-adhesive poly(ionic liquid)-based oral patch for the treatment of oral ulcers with bacterial infection, Acta Biomater. 166 (2023) 254–265.
[9] J.Q. Xing, Y. Ding, X.R. Zheng, P. Yu, M. Qin, R.M. Qiu, Y.Y. Li, S.Y. Shang, J. Xie, J.S. Li, Barnacle-Inspired robust and aesthetic Janus patch with instinctive wet adhesive for oral ulcer treatment, Chem. Eng. J. 444 (2022) 136580.
[10] P. Giunchedi, C. Juliano, E. Gavini, M. Cossu, M. Sorrenti, Formulation and *in vivo* evaluation of chlorhexidine buccal tablets prepared using drug-loaded chitosan microspheres, Eur. J. Pharm. Biopharm. 53 (2) (2002) 233–239.
[11] H. An, Z. Gu, L.P. Zhou, S.Y. Liu, C. Li, M. Zhang, Y.X. Xu, P.X. Zhang, Y.Q. Wen, Janus mucosal dressing with a tough and adhesive hydrogel based on synergistic effects of gelatin, polydopamine, and nano-clay, Acta Biomater. 149 (2022) 126–138.
[12] H. Cao, L.X. Duan, Y. Zhang, J. Cao, K. Zhang, Current hydrogel advances in physicochemical and biological response-driven biomedical application diversity, Signal Transduct. Target. Ther. 6 (1) (2021) 426.
[13] T.C. Ho, C.C. Chang, H.P. Chan, T.W. Chung, C.W. Shu, K.P. Chuang, T.H. Duh, M.H. Yang, Y.C. Tyan, Hydrogels: properties and applications in biomedicine, Molecules 27 (9) (2022) 2902.
[14] J.Y. Li, D.J. Mooney, Designing hydrogels for controlled drug delivery, Nat. Rev. Mater. 1 (12) (2016) 16071.
[15] Y.P. Liang, J.H. He, B.L. Guo, Functional hydrogels as wound dressing to enhance wound healing, ACS Nano 15 (8) (2021) 12687–12722.
[16] X.Y. Li, J.P. Gong, Design principles for strong and tough hydrogels, Nat. Rev. Mater. 9 (2024) 380–398.
[17] H. Lee, S.M. Dellatore, W.M. Miller, P.B. Messersmith, Mussel-inspired surface chemistry for multifunctional coatings, Science 318 (5849) (2007) 426–430.
[18] W. Zhang, R.X. Wang, Z.M. Sun, X.W. Zhu, Q. Zhao, T.F. Zhang, A. Cholewinski, F. Yang, B.X. Zhao, R. Pinnaratip, P.K. Forooshani, B.P. Lee, Catechol-functionalized hydrogels: biomimetic design, adhesion mechanism, and biomedical applications, Chem. Soc. Rev. 49 (2) (2020) 433–464.
[19] Y.J. Fu, Y.F. Shi, L.Y. Wang, Y.F. Zhao, R.K. Wang, K. Li, S.T. Zhang, X.J. Zha, W. Wang, X. Zhao, W. Yang, All-natural immunomodulatory bioadhesive hydrogel promotes angiogenesis and diabetic wound healing by regulating macrophage heterogeneity, Adv. Sci. 10 (13) (2023) 2206771.
[20] B.Y. Lu, X. Han, D. Zou, X. Luo, L. Liu, J.Y. Wang, M.F. Maitz, P. Yang, N. Huang, A.S. Zhao, Catechol-chitosan/polyacrylamide hydrogel wound dressing for regulating local inflammation, Mater. Today Bio 16 (2022) 100392.
[21] Y.C. Lv, F.Y. Cai, Y.X. He, L. Li, Y.F. Huang, J.M. Yang, Y.Q. Zheng, X.A. Shi, Multi-crosslinked hydrogels with strong wet adhesion, self-healing, antibacterial property, reactive oxygen species scavenging activity, and on-demand removability for seawater-immersed wound healing, Acta Biomater. 159 (2023) 95–110.
[22] L.L. Wang, Z.Q. Zhao, J.H. Dong, D.W. Li, W.H. Dong, H.X. Li, Y.Q. Zhou, Q.S. Liu, B.Y. Deng, Mussel-inspired multifunctional hydrogels with adhesive, self-healing, antioxidative, and antibacterial activity for wound healing, ACS Appl. Mater. Interfaces 15 (13) (2023) 16515–16525.
[23] F.P. Deus, A. Ouanounou, Chlorhexidine in dentistry: pharmacology, uses, and adverse effects, Int. Dent. J. 72 (3) (2022) 269–277.
[24] S. Saidin, M.A. Jumat, N.A.A.M. Amin, A.S.S. Al-Hammadi, Organic and inorganic antibacterial approaches in combating bacterial infection for biomedical application, Biomater. Adv. 118 (2021) 111382.
[25] X. Han, B.Y. Lu, D. Zou, X. Luo, L. Liu, M.F. Maitz, P. Yang, N. Huang, A.S. Zhao, J. Chen, Allicin-loaded intelligent hydrogel coating improving vascular implant performance, ACS Appl. Mater. Interfaces 15 (32) (2023) 38247–38263.
[26] P. Yu, Y. Li, H. Sun, H. Zhang, H. Kang, P. Wang, Q. Xin, C. Ding, J. Xie, J. Li, Mimicking antioxidases and hyaluronan synthase: a zwitterionic nanozyme for photothermal therapy of osteoarthritis, Adv. Mater. 35 (2023) 2303299.
[27] Y. Hong, F.F. Zhou, Y.J. Hua, X.Z. Zhang, C.Y. Ni, D.H. Pan, Y.Q. Zhang, D.M. Jiang, L. Yang, Q.N. Lin, Y.W. Zou, D.S. Yu, D.E. Arnot, X.H. Zou, L.Y. Zhu, S.F. Zhang, H.W. Ouyang, A strongly adhesive hemostatic hydrogel for the repair of arterial and heart bleeds, Nat. Commun. 10 (2019) 2060.
[28] B.Y. Lu, D. Luo, A.S. Zhao, H.H. Wang, Y.C. Zhao, M.F. Maitz, P. Yang, N. Huang, pH responsive chitosan and hyaluronic acid layer by layer film for drug delivery applications, Prog. Org. Coat. 135 (2019) 240–247.
[29] Y. Liu, J.M. Teng, R.J. Huang, W. Zhao, D. Yang, Y.X. Ma, H. Wei, H.L. Chen, J.T. Zhang, J. Chen, Injectable plant-derived polysaccharide hydrogels with intrinsic antioxidant bioactivity accelerate wound healing by promoting epithelialization and angiogenesis, Int. J. Biol. Macromol. 266 (2024) 131170.
[30] M.Y. Qu, W.Z. Xu, X.W. Zhou, F. Tang, Q. Chen, X. Zhang, X.F. Bai, Z.Y. Li, X. Jiang, Q.M. Chen, An ROS-scavenging treg-recruiting hydrogel patch for diabetic wound healing, Adv. Funct. Mater. (2024) 2314500.

[31] Y.M. Liu, Detection of LPS-induced macrophage activation with single-cell resolution through DC insulator-based electrokinetic devices, Electrophoresis 44 (11-12) (2023) 978–987.
[32] F.Y. McWhorter, T.T. Wang, P. Nguyen, T. Chung, W.F. Liu, Modulation of macrophage phenotype by cell shape, Proc. Natl. Acad. Sci. USA 110 (43) (2013) 17253–17258.
[33] M.D. Turner, B. Nedjai, T. Hurst, D.J. Pennington, Cytokines and chemokines: at the crossroads of cell signalling and inflammatory disease, BBA-Mol. Cell Res. 1843 (11) (2014) 2563–2582.
[34] P. Conti, G. Ronconi, A. Caraffa, C.E. Gallenga, R. Ross, I. Frydas, S.K. Kritas, Induction of pro-inflammatory cytokines (IL-1 and IL-6) and lung inflammation by Coronavirus-19 (COVI-19 or SARS-CoV-2): anti-inflammatory strategies, J. Biol. Regul. Homeost. Agents 34 (2) (2020) 327–331.
[35] A.S. Tripathy, S. Vishwakarma, D. Trimbake, Y.K. Gurav, V.A. Potdar, N.D. Mokashi, S.D. Patsute, H. Kaushal, M.L. Choudhary, B.N. Tilekar, P. Sarje, V.S. Dange, P. Abraham, Pro-inflammatory CXCL-10, TNF-α, IL-1β, and IL-6: biomarkers of SARS-CoV-2 infection, Arch. Virol. 166 (12) (2021) 3301–3310.
[36] M.S. Huang, Y.S. Huang, H.Y. Liu, Z.M. Tang, Y.X. Chen, Z.J. Huang, S.M. Xu, J.Z. Du, B. Jia, Hydrogels for the treatment of oral and maxillofacial diseases: current research, challenges, and future directions, Biomater. Sci. 10 (22) (2022) 6413–6446.
[37] Y. Li, J.W. Liu, C.X. Lian, H. Yang, M.J. Zhang, Y.F. Wang, H.L. Dai, Bioactive citrate-based polyurethane tissue adhesive for fast sealing and promoted wound healing, Regen. Biomater. 11 (2024) rbad101.
[38] H. Guo, W.J. Zhang, Z.L. Jia, P.H. Wang, Q. Shao, H.F. Shen, J.L. Li, Q. Chen, B. Chi, A biodegradable supramolecular adhesive with robust instant wet adhesion for urgent hemostasis and wound repair, Adv. Funct. Mater. (2024) 2401529.
[39] Y. Qi, C.Y. Xu, Z.D. Zhang, Q. Zhang, Z.Y. Xu, X.R. Zhao, Y.H. Zhao, C.Y. Cui, W.G. Liu, Wet environment-induced adhesion and softening of coenzyme-based polymer elastic patch for treating periodontitis, Bioact. Mater. 35 (2024) 259–273.
[40] W.Y. Zhang, Y.X. He, Y. Chu, Y.X. Zhai, S. Qian, X.H. Wang, P.J. Jiang, P.F. Cui, Y. Zhang, J.H. Wang, Amorphous curcumin-based hydrogels to reduce the incidence of post-surgical intrauterine adhesions, Regen. Biomater. 11 (2024) rbae043.
[41] M. Lee, Y.S. Kim, J. Park, G. Choe, S. Lee, B.G. Kang, J.H. Jun, Y. Shin, M. Kim, Y. Ahn, J.Y. Lee, A paintable and adhesive hydrogel cardiac patch with sustained release of ANGPTL4 for infarcted heart repair, Bioact. Mater. 31 (2024) 395–407.
[42] D. Zhou, S.Z. Li, M.J. Pei, H.J. Yang, S.J. Gu, Y.Z. Tao, D.Z. Ye, Y.S. Zhou, W.L. Xu, P. Xiao, Dopamine-modified hyaluronic acid hydrogel adhesives with fast–forming and high tissue adhesion, ACS Appl. Mater. Interfaces 12 (16) (2020) 18225–18234.
[43] H. Hemmatpour, O. De Luca, D. Crestani, M.C.A. Stuart, A. Lasorsa, P.C.A. van der Wel, K. Loos, T. Giousis, V. Haddadi-Asl, P. Rudolf, New insights in polydopamine formation via surface adsorption, Nat. Commun. 14 (1) (2023) 664.
[44] H. Montazerian, A. Baidya, R. Haghniaz, E. Davoodi, S. Ahadian, N. Annabi, A. Khademhosseini, P.S. Weiss, Stretchable and bioadhesive gelatin methacryloyl-based hydrogels enabled by dopamine polymerization, ACS Appl. Mater. Interfaces 13 (34) (2021) 40290–40301.
[45] L.S. Lin, K.X. Li, F.T. Jiang, D.L. Qiao, B.J. Zhang, F.W. Xie, Towards superior biopolymer gels by enabling interpenetrating network structures: a review on types, applications, and gelation strategies, Adv. Colloid Interface Sci. 325 (2024) 103113.
[46] X. Xue, Y. Hu, S.C. Wang, X. Chen, Y.Y. Jiang, J.C. Su, Fabrication of physical and chemical crosslinked hydrogels for bone tissue engineering, Bioact. Mater. 12 (2022) 327–339.
[47] S. Nejati, L. Mongeau, Injectable, pore-forming, self-healing, and adhesive hyaluronan hydrogels for soft tissue engineering applications, Sci. Rep. 13 (1) (2023) 14303.
[48] C.A. Ghiorghita, I.V. Platon, M.M. Lazar, M.V. Dinu, A.C. Aprotosoaie, Trends in polysaccharide-based hydrogels and their role in enhancing the bioavailability and bioactivity of phytocompounds, Carbohydr. Polym. 334 (2024) 122033.